Technical Physics, 2022, Vol. 67, No. 2

03

Analysis of the response of a liquid surface to the pulse action of an inclined gas jet at low Reynolds number

© *A.P. Savenkov, V.A. Sychev*

Tambov State Technical University,
392000 Tambov, Russia
e-mail: savencow@yandex.ru

Received September 7, 2021
Revised October 31, 2021
Accepted November 4, 2021

A mathematical description of the motion of a cavity on the liquid surface under an oblique action of a gas jet is obtained using the well-known expressions for the movement of a gas bubble in a liquid. The boundary of the viscous drag force domination over the form drag force is determined. The impingement of the gas jet on the liquid surface is considered as a dynamic object of the automatic control theory. It is found that the dynamic properties of the two-phase system „gas jet−liquid" are described by the integrator equations. Using a specially designed setup, the transient response of the „gas jet−liquid" system were experimentally obtained for the aerodynamic action at angles of 20 and 50° to the surfaces of liquids with the viscosities of 0.71 and 26.1 Pa·s (Reynolds number $Re < 2$). The research results are necessary for the analysis of the non-contact aerodynamic method of liquid viscosity measurements.

Keywords: gas jet, impingement, liquid surface, measurement, non-contact, pulse, viscosity.

DOI: 10.21883/TP.2022.02.52944.251-21

Introduction

Metallurgy is the most significant application of processes of gas jet interaction with a liquid [1–6]. A jet, acting on the molten metal surface, plays the key role in chemical transformations and mixing of interacting substances. Interaction of atmospheric-pressure plasma jets with technical and biological liquids is applied for the study of cold plasma properties [7–11]. The shape of a cavity, formed by a gas jet on the liquid surface, is used in optics as a template for the making of aspheric mirrors [12].

Process of gas jet interaction with the liquid surface allow for implementing non-contact measurements of liquid physical properties: density, surface tension and viscosity [13–17]. One of the main prerequisites for application of non-contact methods of liquid properties measurements is their high viscosity (more than 1 Pa·s). When implementing contact methods, viscous liquids cause significant difficulties and time outlays during filling-in of measuring vessels, removal of gas bubbles and cleaning of measuring tools. Non-contact measurement methods, based on deformation of the monitored liquid surface by a gas jet, are the only ones that provide reliable information about viscous liquids' properties [15,17].

Relatively few papers are dedicated to studying the gas jet interaction with the viscous liquid surface ($Re < 1$) [12,14–20]. Inclined impact of a gas jet on the viscous liquid surface allows for generation of stable relaxation oscillations [21]. Oscillations on the surface of a non-viscous liquid ($Re > 100$) are random in nature [2,5,6,10,18,22]. Frequency of oscillations on the viscous liquid surface to a large extent is determined by viscosity, and a non-contact method for measuring this quantity can be based on this dependence. However, the pulse method has a higher measurement accuracy and a wider range [17].

When implementing the non-contact pulse aerohydrodynamic method of viscosity measurements, the surface of the tested liquid is exposed to a gas jet with the formation of a cavity, and the measured quantity is estimated on the basis of the time within which the cavity attains the predefined shape after the beginning of jet impact [17]. The aerodynamic action is stopped before the beginning of relaxation oscillations of the liquid surface. Viscosity is determined using an aperiodic transient response in a two-phase „gas jet−liquid" system, caused by a change in its input parameter – aerodynamic action intensity.

Transient responses of the „gas jet−liquid" system are dealt with in [19,20]. Paper [19] studied the response of the liquid surface to a short aerodynamic pulse after which the inertia force generates a liquid jet. Paper [20] presents the results of computational modeling of a transient responses occurring in a „gas jet−liquid" system under a step perpendicular aerodynamic action (liquid viscosity ~ 1 Pa·s). Interaction of an oblique gas jet with a liquid surface was studied in [3,23–26]. Non-viscous liquids were used in these publications ($Re > 100$).

The task of this paper is a mathematical description of the dynamic properties of a two-phase „gas jet−liquid" system under an inclined aerodynamic action.

1. Theoretical analysis

Computational modeling of occurring processes is often used to study the dynamic interaction of multiphase systems [22,24,26–28]. This approach allows for studying a change in moduli and directions of flow speed vectors in all points of the model of the two-phase system under consideration, but computational modeling results, in their turn, require generalization of the obtained information about the studied system. Simplified approximating equations are required for analysis of system properties [29]. Considerable difficulties for computational modeling are posed by the high viscosity (more than 1 Pa·s) of one of the media. However, computational modeling of a non-viscous liquid also frequently gives unsatisfactory results [6,30].

Our studies are based on the approaches of the automatic control theory. The main dynamic links and a block diagram of a „gas jet–liquid" system have been determined in [29], the dynamic characteristics of these links have been obtained in this paper. Mathematical description of a „gas jet–liquid" system is performed using the known integral expressions for the set of forces acting on the whole region of gas and liquid interaction on the interface.

Fig. 1 shows the images of profile of the cavity on the liquid surface at various time moments from the start of gas jet supply with the interval of 0.4 s. The images have been obtained using the unit described in [31]. A jet was generated by means of a tube, the butt of which is equipped with an discharge orifice (diameter $d = 0.89$ mm and discharge coefficient $\mu = 0.68$). Pressure P upstream of the discharge orifice was maintained at the level of 5.5 kPa in the course of monitoring. The jet discharge orifice is located at distance $H = 10.3$ mm above the liquid surface. The jet acted on the liquid surface at the angle $\alpha = 20°$. The liquid was ED-20 epoxy resin made by „PolyMax" (Saint Petersburg, Russia), dynamic viscosity was $\eta = 11.2$ Pa·s at 27.0°C.

The images in Fig. 1, *b–d* show the formation of a cavity, Fig. 1, *d–h* shows its motion along the liquid surface in the direction of gas jet action, Fig. 1, *g–i* shows the origination of a new cavity, decrease in the volume of the previous cavity and the beginning of relaxation oscillations [21].

Mathematical description of movement of the cavity along the liquid surface should be performed using the equation of force balance on the interface and the known formulas for gas bubble motion in a liquid [10,29,32,33]. The imaginary gas bubble *2* is exposed to the following forces (Fig. 2) [33]:

— F of the gas jet;
— F_σ of surface tension;
— F_ρ of buoyancy;
— F_η of viscous friction;
— F_m of inertia.

The main output signal of a „gas jet–liquid" system under an inclined aerodynamic action is horizontal movement x of the cavity along the liquid surface. The measured quantity is estimated on the basis of the time within which the said quantity attains the predefined value of x_0

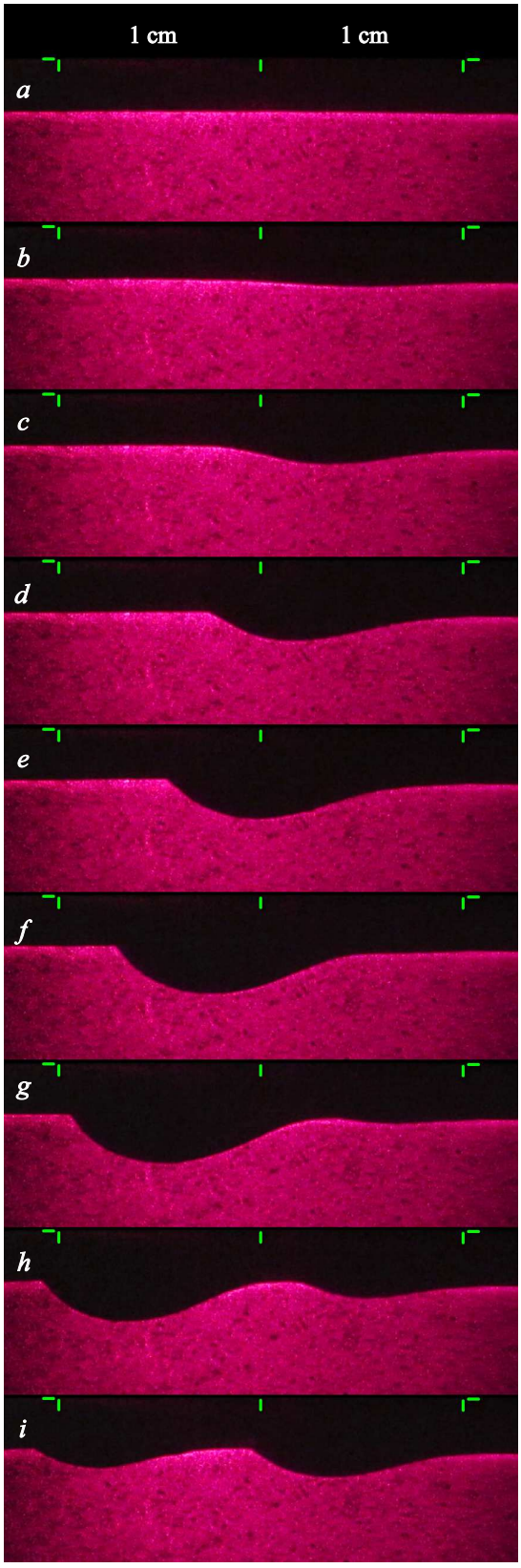

Figure 1. Images of profiles of the cavity on the liquid surface at different time moments from the beginning of gas jet supply: *a–i* — correspond to 0, 0.4, 0.8, 1.2, 1.6, 2.0, 2.4, 2.8, 3.2 s.

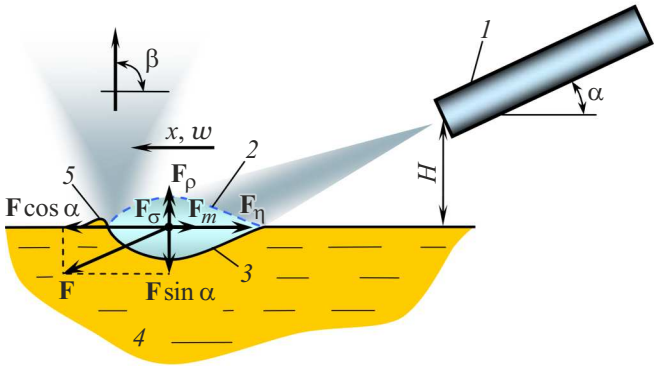

Figure 2. Layout of interaction of a turbulent gas jet with the liquid surface: *1* — jet tube with jet discharge orifice, *2* — imaginary gas bubble, *3* — cavity, *4* — liquid, *5* — wave.

in the non-contact aerohydrodynamic method of viscosity measurement. A projection of the forces onto the horizontal axis provides the corresponding force balance equation

$$F_m + F_\eta = F\cos\alpha. \tag{1}$$

Equation (1) significantly simplifies the processes that take place on the interface. In fact, vertical static forces F_σ and F_ρ affect the cavity size, formation speed and, consequently, the drag coefficient coefficient and motion speed. However, since force F_σ is less than force F_ρ (see [15,29]), while densities of most standard liquids are close to each other, equation (1) gives expressions for describing the cavity motion with an error of percent units.

The force of jet action onto the liquid surface is determined using the formula [29]

$$F = kF_0 = k\,\frac{\pi d^2\mu}{2}\,P, \tag{2}$$

where k — cavity form factor, F_0 — gas momentum flowing out of jet tube *1* per unit time (Fig. 2), [N]. Factor k depends on change in the modulus and direction of the gas momentum vector during gas interaction with the liquid surface. The experiments have shown that gas flows come out of cavity *3* at the mean angle $\beta \approx 90^\circ$ to the liquid surface *4* irrespective of aerodynamic action angle α (in the range $\alpha = 15{-}75^\circ$, Fig. 2). In this case, the direction of gas momentum in a jet due to interaction with the liquid surface changes by angle $90^\circ + \alpha$, while the form factor value is theoretically determined by expression $k = 1 + \sin\alpha$. The corresponding experimental dependence has been obtained in [29]

$$k = A + B\sin\alpha, \tag{3}$$

where $A = 0.54$, $B = 1.33$.

Taking into account (2) and (3), the right-hand member of equation (1) can be rewritten as

$$F\cos\alpha = (A + B\sin\alpha)\cos\alpha\, F_0. \tag{4}$$

Analysis of expression $(A + B\sin\alpha)\cos\alpha$ makes it possible to assume it constant and equal to unity for the angle range $\alpha = 20{-}50^\circ$.

Hydrodynamic drag coefficient to particles motion in a liquid is determined using the formula [33]

$$F_d = C_d\pi R^2\,\frac{\rho w^2}{2}, \tag{5}$$

where C_d — drag coefficient coefficient; R — bubble radius, [m]; w — bubble speed, [m/s]; ρ — liquid density, [kg/m^3]. Viscous drag force F_η prevails in case of a high liquid viscosity and a low particle motion speed ($\mathrm{Re} < 1$). At $\mathrm{Re} < 0.01$, the drag coefficient coefficient of gas bubbles is determined using the formula for solid spherical bodies [34]

$$C_d = \frac{24}{\mathrm{Re}},$$

while formula (5) is converted into the Stokes formula

$$F_\eta = 6\pi R\eta w. \tag{6}$$

As the Reynolds number increases, bubble deformation is observed, the drag coefficient coefficient is affected by gas circulation inside the bubble. With $\mathrm{Re} \approx 1$, the drag coefficient coefficient for gas bubbles is determined using the formula [34]

$$C_d = \frac{16}{\mathrm{Re}}.$$

The direction of gas flows in the cavity is opposite to the direction of gas circulation in the bubble (Fig. 2), which increases the drag coefficient coefficient. The shape of the cavity on the liquid surface also differs from the bubble shape, therefore formula (6) will use the coefficient b_η; its value will be determined as per the experiment data:

$$F_\eta = b_\eta\pi R\eta w. \tag{7}$$

When Reynolds number values significantly exceed one, the contribution of force F_η to the liquid drag force is negligible, while the drag coefficient coefficient tends to one [33]. Strictly speaking, values of C_d in the Reynolds number range of 1 to 100 can be both more than and less than unity [33,34], but we will take $C_d = 1$ for $\mathrm{Re} > 10$ solely to estimate the boundary of domination of the viscous drag force. For the said conditions, we obtain from formula (5) a value of the form drag force, caused by the liquid inertia during flow around the cavity:

$$F_d = \pi R^2\,\frac{\rho w^2}{2}. \tag{8}$$

This paper considers only the case of domination of viscous drag, since interaction of a gas jet with a non-viscous liquid ($\mathrm{Re} > 100$) is random in nature, is accompanied with carryover of splashes and surface oscillations with different frequencies and wavelengths. It is also evident that viscosity can be measured by the non-contact aerohydrodynamic method only when the viscous drag force prevails. Based on

the condition $F_\eta > F_d$, we obtain the maximum permissible Reynolds number value from formulas (6) and (8)

$$\mathrm{Re} = \frac{2Rw\rho}{\eta} < 24. \tag{9}$$

After substituting speed w from formula (6) into condition (9), we obtain the condition of domination of the viscous drag force over the form drag force depending on liquid viscosity —

$$\eta > \sqrt{\frac{F_\eta \rho}{72\pi}} \approx 0.066\sqrt{F_\eta \rho}. \tag{10}$$

Force F of gas jet action can be used to estimate the boundary value of viscosity in formula (10), since viscous drag force F_η is the main counteracting force. The images in Fig. 1 have been obtained in experimental conditions, under which force F was ~ 4 mN. For this force value, we obtain the boundary viscosity value $\eta \approx 0.13$ Pa·s from expression (10). With smaller viscosity values, inertia force F_m in equation (1) shall include a term responsible for action of the form drag force.

When liquid viscosity exceeds the boundary value of 0.13 Pa·s, inertia force F_m is determined by acceleration of the added mass of the cavity. The inertia force for a spherical gas bubble with radius R can be estimated using the formula [33]

$$F_m = \frac{2}{3}\pi R^3 \rho \frac{d^2x}{dt^2}, \tag{11}$$

where t is time, [s]. Coefficient b_m will be subsequently used in formula (11) instead of value 2/3 in order to take into account asphericity of the cavity on the liquid surface and other factors.

Only half the surface of the bubble *2* is in contact with liquid *4* (Fig. 2). Expressions (7) and (11) should be divided by 2 when substituting forces F_η and F_m into equation (1). Taking into account expression (4), we get a differential equation from force balance equation (1)

$$\frac{1}{2} b_m \pi R^3 \rho \frac{d^2x}{dt^2} + \frac{1}{2} b_\eta \pi R \eta \frac{dx}{dt} = F_0. \tag{12}$$

The initial conditions for solving this equation are

$$x(0) = x^0, \quad x'(0) = 0, \tag{13}$$

where x^0 is the cavity position at the time of its formation, [m].

A transfer function is obtained from equation (12) after a Laplace transformation

$$W(s) = \frac{x(s)}{F_0(s)} = \frac{2}{b_m \pi R^3 \rho s^2 + b_\eta \pi R \eta s},$$

where s is the Laplace transformation parameter, [s^{-1}], and it is reduced to the common form

$$W(s) = \frac{K}{s(Ts+1)}, \tag{14}$$

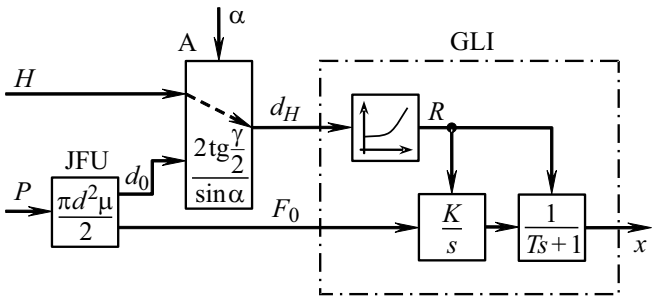

Figure 3. Block diagram of the two-phase „gas jet−liquid" system under an inclined aerodynamic action: JFU — Jet Forming Unit; A — Atmosphere; GLI — Gas−Liquid Interface.

where $K = 2/(b_\eta \pi R \eta)$ — transfer factor, [s/kg]; $T = b_m R^2 \rho/(b_\eta \eta)$ — time constant, [s].

Similarly to [29], we present the results of the theoretical analysis of a two-phase „gas jet−liquid" system under an inclined aerodynamic action in the form of a block diagram (Fig. 3).

Potential energy of compressed gas (excess pressure P) is converted by the jet forming unit (JFU) into kinetic energy of a jet with momentum F_0 per unit time and diameter $d_0 < d$. Fig. 3 shows for the JFU link the transfer factor for the $P-F_0$ channel. The gas jet interacts with atmospheric air (A), which results in a linear increase of the jet diameter (as distance from the JFU increases) up to the value d_H near the liquid surface. Momentum F_0 does not change.

Diameter d_0 hardly affects diameter d_H since distance H significantly exceeds d_0 [35]. The transfer factor for the $H-d_H$ channel is shown for link A. Angle γ of cone of turbulent jets, flowing out of a thin plate orifice, does not much depend on Reynolds number. At present, angle γ is usually determined for a cone on whose surface the gas motion speed is equal to half the axial speed. According to [35,36] the value of this angle is 5°. When distance H is constant, JFU inclination angle α affects the length of free gas flow up to the gas-liquid interface (GLI), and, consequently, it affects diameter d_H.

Differential equation (12) and transfer function (14) describe the dynamic characteristics of a GLI object represented as a series connection of an integrator and an aperiodic link. The integrator with transfer function K/s corresponds to counteraction of viscous drag force F_η against movement of the cavity, the aperiodic link — to counteraction of inertia force F_m of the added mass of the cavity at the time of gas jet supply till achievement of a constant motion speed. Cavity radius R affects operation of these dynamic links, since it is included in the formulas for determination of their parameters K and T. The relationship between radius R and diameter d_H is presented as an abstract nonlinear link, since at present no physically justified mathematical dependence is known to adequately describe this relationship. When values of d_H are small, radius R does not become zero thanks to the action of

surface tension. Values of radius R in particular conditions are determined experimentally.

The integrator is astatic. According to the predefined mathematical description and the block diagram of the „gas jet–liquid“system, the cavity will move to an infinitely great distance until the gas jet is acting. In fact, significant movement of the cavity is hindered by internal feedback, under the action of which a new cavity appears and the old one disappears. A relaxation oscillation is observed. The mechanism of the oscillatory condition of gas jet interaction with a liquid surface is described in detail in [21]. Study of feedbacks in a „gas jet–liquid“ systems is outside the scope of this paper, since the jet impact during implementation of the considered pulse aerohydrodynamic method of viscosity measurements is stopped until the oscillatory process begins. The block diagram (Fig. 3) does not show the corresponding feedbacks.

By substituting formula (2) into equation (12), we obtain a differential equation of the „gas jet–liquid“ system for the $P-x$ channel:

$$\frac{b_m R^3 \rho}{\mu d^2}\frac{d^2x}{dt^2} + \frac{b_\eta R \eta}{\mu d^2}\frac{dx}{dt} = P \qquad (15)$$

with initial conditions (13). Equation (15) can be solved to determine the transient response of the „gas jet–liquid“ system as a response to a step pneumatic action of type $P \cdot 1(t)$, where $1(t)$ is the Heaviside function. The transient response equation is

$$x(t) = x^0 + \frac{b_m R \rho \mu d^2 P}{b_\eta^2 \eta^2}\left[\exp\left(-\frac{b_\eta \eta}{b_m R^2 \rho}t\right) - 1\right] + \frac{\mu d^2 P}{b_\eta R \eta}t. \qquad (16)$$

The first term in this function is determined by the reference point of cavity movement x, the second item is responsible for the action of inertia force F_m, and the third item — for the action of viscous drag force F_η. Let us estimate significance of the exponent in function (16). Let us define $b_\eta = 6$, $b_m = 2/3$, $\rho = 1000\,\mathrm{kg/m^3}$ and use the known experiment data for the boundary viscosity value $\eta = 0.13\,\mathrm{Pa{\cdot}s}$ (see formula (10)): radius $R = 5\,\mathrm{mm}$ and deformation time $t = 0.1\,\mathrm{s}$. We obtain an exponent value of 0.009. The exponent value for $\eta = 0.3\,\mathrm{Pa{\cdot}s}$ is below 10^{-4}, which is considerably less than unity. Consequently, the expression in square brackets in function (16) for the viscosity range under study can be taken equal to minus unity. The linear transient response is obtained from function (16)

$$x(t) = x^0 - \frac{b_m R \rho \mu d^2 P}{b_\eta^2 \eta^2} + \frac{\mu d^2 P}{b_\eta R \eta}t. \qquad (17)$$

When viscosity is 2 Pa·s, the second term in function (17) takes on the value of 0.068 mm and falls drastically as viscosity increases (the above-mentioned values of the quantities are used for the calculation). This makes it possible to present the transient response for viscous liquids in a simplified form

$$x(t) = x^0 + \frac{\mu d^2 P}{b_\eta R \eta}t. \qquad (18)$$

2. Experimental part

A setup shown in Fig. 4 was used for an experimental check of the conducted theoretical research and for determination of the actual values of coefficients b_m and b_η. Strip *2*, whereon jet tube *1* with a discharge orifice (diameter $d = 0.89\,\mathrm{mm}$ and discharge coefficient $\mu = 0.68$), guide *3* and ruler *4* are fastened, is placed above the surface of liquid *11* in vessel *8*. The printed board of the laser triangulation detector (TD) [37] of liquid surface can move horizontally along guide *3*. Drive D is used for vertical motion of elements *1–7* and TD.

Compressed air from the pneumatic supply line is fed into jet tube *1* via pressure-reducing valve Z of type RDV5M, solenoid valve Y of type P1PR.5 and laminar-flow restrictor R (pneumatic drag coefficient). Pressure P in the jet tube is controlled by valve Z and is monitored according to readings of pressure gauge M (type M-1/4) and calibrated pressure transducer PT (type MPX5010DP). Receiver T is intended for reduction of supply pressure

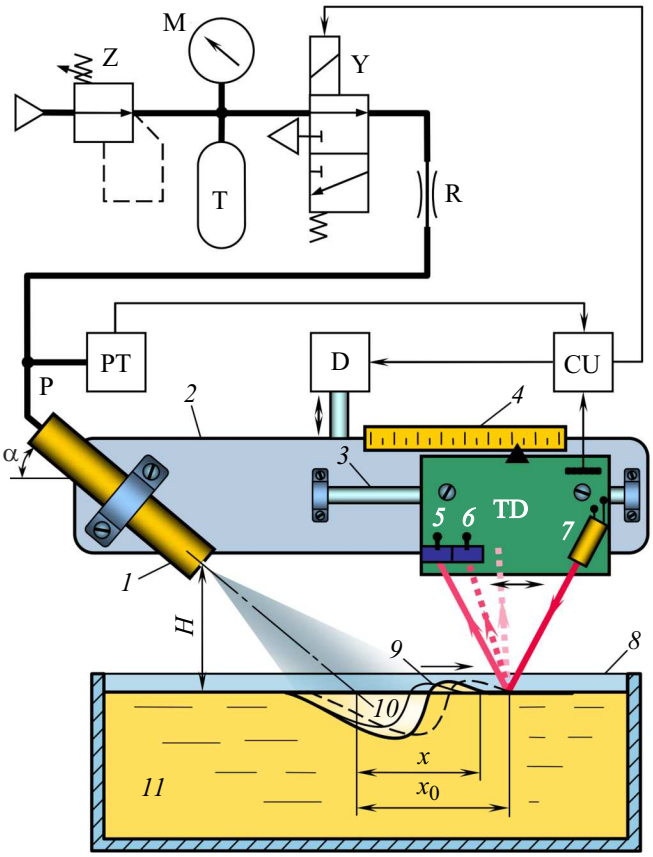

Figure 4. Layout of an experimental setup for studying the gas jet interaction with the liquid surface (the designations in the figure are explained in the text).

pulsations at switchovers of solenoid valve Y. Operation of the setup is controlled by means of control unit CU based on the ATmega16A microcontroller.

TD is intended for automatic setting of jet tube *1* to the predefined distance H in relation to liquid surface *11* and for detection of its deformation by the gas jet at the predefined point. Operation of the setup is described in [17], TD — in [37].

The setup allows for determination of time within which the wave *9* attains the predefined movement x_0. Movement x of wave *9* is counted from the point of intersection of the gas jet axis with the plane of the undeformed liquid surface *11* and up to the point of incidence of the laser diode beam *7* onto it. When the corresponding button of control unit CU is pressed, distributor Y opens, counting of jet action time t begins and continuous measurement of pressure P by means of transducer PT starts. The gas jet, flowing out of jet tube *1*, forms a cavity *10* with wave *9*. The cavity moves in the direction of jet action and deflects the reflected beam of the laser diode *7* when movement x_0 is reached. When the beam passes from the surface of photodiode *5* to the surface of photodiode *6*, distributor Y closes, counting of jet action time t stops and the average value of pressure P for the predefined time is determined. The obtained values of t and P are output to the display of control unit CU. If necessary, pressure P is adjusted by means of valve Z.

For experimental determination of transient response $x(t)$, gas jet action time t is measured many times at different predefined values x_0 of movement x. A change in x_0 is implemented by moving the TD along horizontal guide *3* and is monitored using ruler *4*.

The experiments have been carried out using DAB-10 castor oil ($\eta = 0.710$ Pa·s, $\rho = 957$ kg/m^3) made by AMEE CASTOR & DERIVATIVES LTD (Banaskantha, India) and ED-20 epoxy resin ($\eta = 26.1$ Pa·s, $\rho = 1123$ kg/m^3) made by LTD Holding Company „FEM“ (Dzerzhinsk, Russia) at the temperature of 25.0 ± 0.1°C for the angle α of 20 and 50°. Viscosity was determined using a calibrated Brookfield viscometer (model LVF), density — by the picnometer method. The value of distance H at $\alpha = 20°$ was taken equal to 10.3 mm, at $\alpha = 50° - 16.7$ mm.

3. Results and discussion

Fig. 5 shows the experimental transient responses $x(t)$ of the „gas jet–liquid“system. The positions of the plots along the abscissa axis at different values of pressure P and viscosity η were maintained using the dimensionless time parameter

$$t^* = \frac{P}{\eta} t.$$

All the dependences in Fig. 5, *a* have been plotted at $P = 5.5$ kPa.

Fig. 5, *a* shows the data for ED-20 epoxy resin obtained by means of the experimental setup (Fig. 4) and according

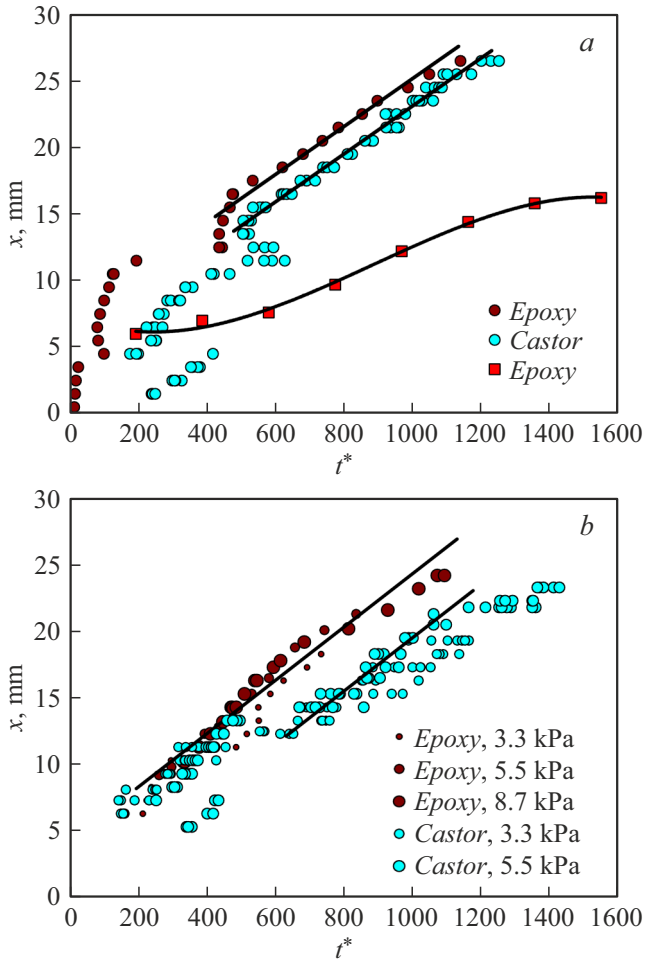

Figure 5. Transient responses of the „gas jet–liquid“ system for angle $\alpha = 20$ (*a*) and $\alpha = 50°$ (*b*): • – obtained by means of an experimental setup (Fig. 4), ■ — obtained by processing of the cavity images (Fig. 1), the lines show the approximation results.

to the results of cavity image analysis (Fig. 1). These dependences differ from each other by size of wave *9* (Fig. 4). Using the images in Fig. 1, movement x is determined according to the point of cavity profile intersection with the undeformed liquid surface. The setup (Fig. 4) allows for determination of x according to the wave front *9*. All the approximating lines at $t = 0$ converge to distance $x \approx 6$ mm, which correspond to the cavity radius at the beginning of liquid surface deformation.

The experimental dependences, obtained using the setup (Fig. 4), have typical gaps. This is due to the fact that the TD beam at $x = 0-6$ mm falls on the surface of originating cavity *10*, while at $x = 6-15$ mm it falls on different points of the surface of originating wave *9* (Fig. 4). The data that reflects movement of the cavity along the liquid surface corresponds to range $x = 15-27$ mm. This range for the data predefined in Fig. 5, *b* corresponds to $x = 14-25$ mm. Cavity motion speed beyond the upper limits of these ranges decreases since a part of gas momentum in the jet is spent for the formation of a new cavity (Fig. 1).

Results of approximation of the transient responses of the gas jet–liquid system by function (18)

α	η, Pa·s	P, kPa	Range, mm	x^0, mm	Δx, mm	σx, mm	δx, %
20°	0.71	5.45	14–26	5.1	0.9	0.4	2.0
	26.1	5.45	14–27	7.2	1.2	0.6	2.8
50°	0.71	5.45	14–21	−0.4	2.4	0.9	5.2
	26.1	3.27 5.45 8.71	14–18 9–21 10–24	4.4	2.0	0.9	5.5

Note: Δx — maximum absolute deviation of experimental data from function (18); σx — root-mean-square deviation of experimental data; δx — relative approximation error.

The experimental data obtained using the setup (Fig. 4) have been approximated by function (18), the data obtained from the images in Fig. 1, — by a random cubic polynomial. The data for castor oil at $\alpha = 50°$ and $P = 3.3$ kPa was not approximated due to their significant difference from the other data. All the data for epoxy resin at $\alpha = 50°$ were approximated by one function.

All the approximating functions (18) used a theoretical value of coefficient $b_\eta = 6$. Half the maximum cross-sectional size of the cavity in the plane of the undeformed liquid surface was used as radius R. The values of radius R were determined according to the cavity images in the vertical plane perpendicular to the plane where the images were obtained (shown in Fig. 1). The radius values of 5.0 and 4.5 mm respectively have been obtained for angles α equal to 20 and 50°. The single parameter x^0 was determined as a result of approximation.

The table gives the results of approximation of the transient responses of the „gas jet–liquid„ system by function (18). The values of x^0 for castor oil are lesser than for epoxy resin. Assuming that the difference of these values is equal to the second summand in function (17), the values of coefficient b_m were determined. The values of b_m equal to 3.3 and 6.6 mm respectively have been obtained for angles α equal to 20 and 50°, the theoretical value being 0.67 (see formula (11)). Evidently, such exceeding of the theoretical value of coefficient b_m can be only partially explained by the cavity shape deviation from the spherical one (Fig. 2). The most probable reason for a leftward shift of the transient responses is a transient process in the setup upon opening of distributor Y (Fig. 4). Pressure upstream of the discharge orifice increases exponentially (first-order aperiodic link) with time constant ~ 50 ms. The experiment is conducted so that the average pressure values for the jet action period are equal to the above-mentioned ones (3.3 and 5.5 kPa), however, the beginning of the aerodynamic action is significantly weaker than its end.

Another probable reason for an increase in coefficient b_m as compared to the theoretical value is the opposite direction of gas circulation in the cavity formed by a gas jet on the liquid surface, in relation to the gas circulation direction in a rising gas bubble. Gas motion along the interface in the cavity causes a stronger liquid flow in the direction of cavity motion than the liquid flow around a rising gas bubble having the same volume.

Despite the fact that the experimental value of coefficient b_m does not match the theoretical one, the results of the mathematical description of cavity motion are satisfactory. When viscosity changes in 37 times and density changes in 1.2 times, the average deviation of x values for different liquids from each other is 10% at $\alpha = 20$ and 30% at $\alpha = 50°$.

Interaction of an inclined gas jet with the liquid surface better corresponds to theoretical analysis at small inclination angles (20°). This manifests itself in a greater range of linear movement of the cavity and a smaller approximation error.

Conclusion

The following conclusions can be made based on the results of the theoretical and experimental studies of transient responses of the two-phase „gas jet–liquid“ system.

A mathematical description of cavity motion along the liquid surface can be successfully performed using the known expressions for the forces acting on a moving gas bubble. Thereat, the coefficient in the Stokes formula should be taken equal to the theoretical value *6*. The dependence of this coefficient on various factors should be studied using a setup where detection of a deformation by the triangulation detector triggers movement of the device elements in parallel to the liquid surface in the direction of the gas jet action.

The boundary viscosity value, which determines domination of the viscous drag force over the form drag force, depends only on the force of gas jet action onto the liquid surface and on liquid density. The boundary viscosity value in the considered conditions was 0.13 Pa·s (Re = 24).

The „gas jet–liquid“ system is described by integrator equations, which is confirmed by the presence of linear segments in the transient response plots. The best possible fit of the theory is observed at small angles of aerodynamic action.

The obtained equations for the transient responses of the „gas jet–liquid“ system can be used to determine the lower

limit, model and function of liquid viscosity measurements by the non-contact aerohydrodynamic method. The used mathematical dependences and approaches to obtaining them make it possible to conduct further research of the two-phase „gas jet–liquid“system, in particular, in the condition of stable relaxation oscillations.

Conflict of interest

The authors declare that they have no conflict of interest.

References

[1] N. Dyussekenov, S.S. Park, H.Y. Sohn. Miner. Process. Extr. M., **120** (1), 21 (2011). DOI: 10.1179/037195510X12791826058136
[2] J. Maruyama, K. Ito, M. Ando, J. Okada, K. Ito. ISIJ Int., **60** (6), 1375 (2020). DOI: 10.2355/isijinternational.ISIJINT-2019-653
[3] Y. Chen, A.K. Silaen, C.Q. Zhou. Processes, **8** (6), 700 (2020). DOI: 10.3390/pr8060700
[4] G.Q. Liu, G.X. Zhang, K. Liu. Metalurgija, **59** (3), 299 (2020).
[5] S. Sabah, G. Brooks. Ironmaking & Steelmaking, **43** (6), 473 (2016). DOI: 10.1080/03019233.2015.1113755
[6] D. Muñoz-Esparza, J.-M. Buchlin, K. Myrillas, R. Berger. Appl. Math. Model., **36** (6), 2687 (2012). DOI: 10.1016/j.apm.2011.09.052
[7] C.J. Ojiako, R. Cimpeanu, H.C.H. Bandulasena, R. Smith, D. Tseluiko. J. Fluid Mech., **905**, A18 (2020). DOI: 10.1017/jfm.2020.751
[8] B.B. Baldanov, A.P. Semenov, Ts.V. Ranzhurov, E.O. Nikolaev, S.V. Gomboeva. Tech. Phys., **60** (11), 1729 (2015). DOI: 10.1134/S1063784215110043
[9] A. Stancampiano, E. Simoncelli, M. Boselli, V. Colombo, M. Gherardi. Plasma Sourc. Sci. Tech., **27** (12), 125002 (2018). DOI: 10.1088/1361-6595/aae9d0
[10] S. Park, W. Choe, H. Lee, J.Y. Park, J. Kim, S.Y. Moon, U. Cvelbar. Nature, **592**, 49 (2021). DOI: 10.1038/s41586-021-03359-9
[11] T.R. Brubaker, K. Ishikawa, H. Kondo, T. Tsutsumi, H. Hashizume, H. Tanaka, S.D. Knecht, S.G. Bilén, M. Hori. J. Phys. D: Appl. Phys., **52** (7), 075203 (2018). DOI: 10.1088/1361-6463/aaf460
[12] W. Fu, X. Zhang. Optik, **207**, 164451 (2020). DOI: 10.1016/j.ijleo.2020.164451
[13] D.M. Mordasov, M.M. Mordasov. Tech. Phys., **62** (3), 490 (2017). DOI: 10.1134/S1063784217030148
[14] A.H. Pfund, E.W. Greenfield. Ind. Eng. Chem., **8** (2), 81 (1936). DOI: 10.1021/ac50100a001
[15] M.M. Mordasov, A.P. Savenkov, M.E. Safonova, V.A. Sychev. Meas. Tech., **61** (6), 613 (2018). DOI: 10.1007/s11018-018-1473-7
[16] B.V. Deryagin, V.V. Karasev, Russ. Chem. Rev., **57** (7), 634 (1988). DOI: 10.1070/RC1988v057n07ABEH003379
[17] A.P. Savenkov, M.M. Mordasov, V.A. Sychev. Meas. Tech., **63** (9), 722 (2020). DOI: 10.1007/s11018-021-01845-0
[18] A. He, A. Belmonte. Phys. Fluid., **22** (4), 042103 (2010). DOI: 10.1063/1.3327209
[19] É. Ghabache, T. Séon, A. Antkowiak. J. Fluid. Mech., **761**, 206 (2014). DOI: 10.1017/jfm.2014.629
[20] A. Balabel. Emirates J. Engineer. Res., **12** (3), 35 (2007).
[21] M.M. Mordasov, A.P. Savenkov. Tech. Phys. Lett., **42** (9), 940 (2016). DOI: 10.1134/S1063785016090224
[22] M. Adib, M.A. Ehteram, H.B. Tabrizi. Appl. Math. Model., **62**, 510 (2018). DOI: 10.1016/j.apm.2018.05.031
[23] R.D. Collins, H. Lubanska. Brit. J. Appl. Phys., **5** (1), 22 (1954). DOI: 10.1088/0508-3443/5/1/306
[24] J. Solórzano-López, R. Zenit, M.A. Ramírez-Argáez. Appl. Math. Model., **35** (10), 4991 (2011). DOI: 10.1016/j.apm.2011.04.012
[25] O. McRae, A. Gaillard, J.C. Bird. Phys. Rev. E, **96** (1), 013112 (2017). DOI: 10.1103/PhysRevE.96.013112
[26] X.-T. Wu, R. Zhu, G.-S. Wei, K. Dong. J. Min. Metall. B, **56** (3), 307 (2020). DOI: 10.2298/JMMB190225019W
[27] R.B. Kalifa, S.B. Hamza, N.M. Saïd, H. Bournot. Int. J. Mech. Sci., **165**, 105220 (2020). DOI: 10.1016/j.ijmecsci.2019.105220
[28] X. Zhou, Q. Yue, Z. Di, D. Sheng, M. Ersson. JOM, **73** (10), 2953 (2021). DOI: 10.1007/s11837-021-04810-y
[29] M.M. Mordasov, A.P. Savenkov, K.E. Chechetov. Tech. Phys., **61** (5), 659 (2016). DOI: 10.1134/S1063784216050170
[30] V.N. Petrov, A.S. Shabalin, V.F. Sopin, S.B. Petrov, S.L. Malyshev. Vestn. tekhnolog. un-ta, **20** (2), 85 (2017) (in Russian).
[31] M.M. Mordasov, A.P. Savenkov. Meas. Tech., **58** (7), 796 (2015). DOI: 10.1007/s11018-015-0796-x
[32] V.A. Makarov, F.A. Korolev, R.E. Tyutyaev. IOP Conf. Ser.: Mater. Sci. Eng., **1047**, 012014 (2021). DOI: 10.1088/1757-899X/1047/1/012014
[33] P. Snabre, F. Magnifotcham. Eur. Phys. J. B Condens. Matter., **4** (3), 369 (1998). DOI: 10.1007/s100510050392
[34] G.I. Kelbaliyev. Theor. Found. Chem. Eng., **45** (3), 248 (2011). DOI: 10.1134/S0040579511020084
[35] W.R. Quinn. Eur. J. Mech. B/Fluids, **25** (3), 279 (2006). DOI: 10.1016/j.euromechflu.2005.10.002
[36] J. Mi, P. Kalt, G.J. Nathan, C.Y. Wong. Exp. Fluid., **42** (4), 625 (2007). DOI: 10.1007/s00348-007-0271-9
[37] M.M. Mordasov, A.P. Savenkov, M.E. Safonova, V.A. Sychev. Optoelectron., Instrum. Data Process., **54** (1), 69 (2018). DOI: 10.3103/S8756699018010119